Available online at www.sciencedirect.com
SCIENCE DIRECT®
European Journal of Mechanics B/Fluids 25 (2006) 153–163

Dynamical system based optimal control of incompressible fluids. Boundary control

Yulian Spasov [1], Karl Kunisch *

Institut für Mathematik, Karl-Franzens-Universität Graz, Heinrichstrasse 36, A-8010 Graz, Austria

Received 6 January 2004; received in revised form 31 March 2005; accepted 23 June 2005

Available online 28 October 2005

Abstract

The choice of the cost functional for vortex reduction in optimal control of fluid flow is still an important challenge. We propose to utilize a dynamical systems based measure for vorticity involving the velocity gradient tensor in the cost functional. Its effectiveness and some of its features are demonstrated for boundary control problems.

Keywords: Optimal control; Incompressible flow; Dynamical systems

1. Introduction

The goal of this short paper is to propose an optimal control formulation for vortex reduction by means of boundary control and to demonstrate its numerical feasibility. To partially set the stage consider the cost functional of the form

$$\min J(\mathbf{y}, \mathbf{u}) = J_1(\mathbf{y}) + J_2(\mathbf{u}), \tag{1}$$

which is minimized subject to the Navier Stokes equations. Here $\mathbf{y} = \mathbf{y}(t, \mathbf{x})$ denotes the velocity vector of the fluid at time $t > 0$ and location $\mathbf{x}$ in the spatial domain Ω, and $\mathbf{u}$ stands for the boundary control variable chosen from a space U of admissible controls. The control variables may represent blowing or suction along the boundary. In many cases a proper choice for J_2 is given by

$$J_2(\mathbf{u}) = \int_0^T \int_{\Gamma_c} \left|\mathbf{u}(t, \mathbf{x})\right|^2 \mathrm{d}\mathbf{x}\,\mathrm{d}t, \tag{2}$$

where $T > 0$ denotes the control horizon and Γ_c is the part of the boundary Γ of Ω along which control is applied.

The choice of J_1 is significantly more delicate. In fact, the quantification of vorticity is a research area in its own right. To explain the approach let $A = \nabla\mathbf{y}(t, \mathbf{x})$ stand for the velocity gradient tensor at $(t, \mathbf{x})$ and introduce its

* Corresponding author.
E-mail address: karl.kunisch@uni-graz.at (K. Kunisch).
[1] Present address: Swinden Technology Centre, Corus, Rotherham, S60 3AR, UK.

0997-7546/$ – see front matter
doi:10.1016/j.euromechflu.2005.06.004

symmetric and antisymmetric parts $S = \frac{1}{2}(A + A^{\mathrm{T}})$ and $T = \frac{1}{2}(A - A^{\mathrm{T}})$, referred to as strain and rotation tensor respectively. For three-dimensional flows the characteristic equation for A is given by

$$\lambda^3 - (\operatorname{tr} A)\lambda^2 + \frac{1}{2}\big((\operatorname{tr} A)^2 - \operatorname{tr} A^2\big)\lambda - \det A = 0,$$

where $\operatorname{tr} A$ denotes the trace of A. For incompressible fluids $\operatorname{tr} A = 0$ and the characteristic equation reduces to

$$\lambda^3 - \frac{1}{2}\operatorname{tr} A^2\lambda - \det A = 0,$$

with associated discriminant D given by

$$D = \left(\frac{1}{2}\det A\right)^2 - \frac{1}{216}(\operatorname{tr} A^2)^3.$$

If $D > 0$ then A has one real and two complex eigenvalues. Based on these quantities and local dynamical systems analysis of $\dot{\mathbf{x}} = A\mathbf{x}$, various definitions for the existences of vortices in fluids were proposed and analyzed. In [1,2] vortex cores are related to regions with complex eigenvalues of $\nabla\mathbf{y}$. In terms of linear dynamical systems complex eigenvalues correspond to centers and foci, see [3]. In [4] an eddy is defined as a region where $-\operatorname{tr} A^2$ is positive with pressure which is below an ambient value. The third definition is based on the strain and rotational tensors and defines a vortex core as a connected region within which the symmetric matrix $S^2 + T^2$ has two negative eigenvalues, [5]. Respective merits and differences among the three definitions are analyzed in [5].

In the two dimensional case the definitions explained so far coincide and a vortex is predicted in regions where the eigenvalues of A are complex or equivalently, where

$$\det \nabla\mathbf{y}(t, \mathbf{x}) > 0. \tag{3}$$

We aim for an optimal control formulation with vortex reduction as control objective. This suggests the cost functional

$$J_1(\mathbf{y}) = \int_0^T \int_{\Omega_0} h\big(\det \nabla\mathbf{y}(t, \mathbf{x})\big)\,\mathrm{d}\mathbf{x}\,\mathrm{d}t, \tag{4}$$

where Ω_0 denotes the spatial region within which vortex reduction is desired, T is the control horizon, and $h : \mathbb{R} \to \mathbb{R}^+$ is a nonnegative C^1-function, which penalizes $\nabla\mathbf{y}(t, \mathbf{x}) > 0$. A possible choice for h is given by

$$h(s) = \begin{cases} 0 & \text{if } s < -\delta, \\ \frac{s^2}{2\delta} + s + \frac{\delta}{2} & \text{if } -\delta \leqslant s \leqslant 0, \\ s + \frac{\delta}{2} & \text{if } 0 \leqslant s, \end{cases} \tag{5}$$

for a fixed, small $\delta > 0$. Note that we chose to regularize h to the left of the origin. Alternatively we could have chosen $h = 0$ on $(-\infty, 0]$ which would have implied relatively small values of h for small $s > 0$, which we want to avoid.

Historically the above quantifications were preceded by the *Q-criterion* of Hunt, Wray and Moin [4] which defines a vortex as a region where $|T|^2 + |S|^2 > 0$. In two spatial dimensions the same criterion is known as the Okubo–Weiss criterion [6,7]. All the criteria discussed so far are Galilean invariant, i.e. they remain invariant under coordinate changes of the form $\mathbf{y} = \mathbf{Q}\mathbf{x} + \mathbf{a}t$, where $\mathbf{Q}$ is a proper orthogonal tensor and $\mathbf{a}$ is a constant velocity vector. In a recent paper by Haller [8] it is argued that Galilean invariance is not sufficient and that proper definitions must be *objective*, i.e. they must be invariant under transformations of the form $\mathbf{y} = \mathbf{Q}(t)\mathbf{x} + \mathbf{a}(t)$. In [8] a vortex is defined as a set of fluid trajectories along which the strain acceleration tensor is indefinite over directions of zero strain.

The choice of J_1 as a measure for penalizing vorticity, presents a distinct departure from commonly used cost functionals in optimal control with drag or vorticity reduction as control objective. We have shown it effectiveness for distributed control in [9]. A frequently used functional is of the form $J_1(\mathbf{y}) = \int_0^T \int_{\Omega_0} |\operatorname{curl}\mathbf{y}|^2$, see e.g. [10–13] and the references given there. The short-coming of using $\operatorname{curl}\mathbf{y}$ for measuring vorticity include that it does not identify vortex cores in shear flow, especially if the background shear is comparable to the vorticity within the vortex [5]. An alternative choice of cost functional is given by the tracking functional $J_1(\mathbf{y}) = \int_0^T \int_{\Omega_0} |\mathbf{y} - \mathbf{y}_{\mathrm{Stokes}}|^2$, where $\mathbf{y}_{\mathrm{Stokes}}$ denotes the solution to the Stokes problem with all other specifications as for the nonlinear flow [13–15]. The control problem then consists in determining a control for the nonlinear flow which in the least squares sense optimally

approximates the Stokes flow. One of the advantages of this formulation is given by the fact that the second order sufficient optimality conditions will be satisfied if the controlled nonlinear flow and the linear flow are sufficiently close.

The focus of this work is to utilize an adequate functional for open loop vortex reduction. Our cost functional is Galilean invariant, all previously used ones are not. Certainly it would be of tremendous interest to investigate control strategies which are stable with respect to system perturbations. This requires closed loop control strategies which, in the context of nonlinear equations, involve the Hamilton Jacobi Bellman (HJB) equation. Due to the well-known curse of dimensionality it is at present out of scope to numerically treat the HJB equation in the context of control of the Navier–Stokes equations. In an independently conduced research [16] we combined model reduction techniques with the HJB approach to design robust feedback laws for nonlinear equations. It would certainly be of interest to utilize the techniques developed in [8] for Galilean invariant cost functionals for vortex reduction.

Note also that care must be exercised in evaluating the success of an optimal control strategy to suppress vortices. It is tempting to use graphical methods comparing the controlled and uncontrolled flows on the basis of local pressure minima or path-line and streamline formation. In general such approaches are inadequate for detecting and comparing vortices in an unsteady flow [5]. From a numerical point of view one will monitor the value of J, J_1 and J_2 during an iterative procedure for solving (1). If one starts with the uncontrolled flow then J and J_1 must decrease and $|\nabla J|$ must converge to 0 as the iteration proceeds. In our numerical experiments β is chosen such that J_1 is of approximately the same magnitude as βJ_2 at the converged values.

Section 2 contains a precise problem statement and the adjoint-based optimality system. It provides the gradient for the iterative optimization method to solve the optimal control problem. In Section 3 we first specify the numerical methods that are utilized. Subsequently these methods are tested before we turn to a description of the numerical tests for boundary control.

2. Adjoint based and numerical optimal control

Let Ω be a bounded spatial two-dimensional domain with boundary Γ. By $\mathbf{y} = (y_1, y_2)$ we denote the velocity of the fluid in the directions $\mathbf{x} = (x_1, x_2)$ and p denotes its pressure. The controlled time-dependent Navier–Stokes equations on the time-space cylinder $Q = (0, T) \times \Omega$, $T > 0$, are given by

$$\mathbf{y}_t - \frac{1}{Re}\Delta\mathbf{y} + (\mathbf{y} \cdot \nabla)\mathbf{y} + \nabla p = 0 \quad \text{in } Q, \tag{6a}$$

$$-\operatorname{div}\mathbf{y} = 0 \quad \text{in } Q, \tag{6b}$$

where Δ denotes the component-wise Laplacian $\sum_{j=1}^{2} \partial^2 y_i / \partial x_j^2$, $(\mathbf{y} \cdot \nabla)\mathbf{y}$ stands for the vector with components $\sum_{j=1}^{2} y_j \partial y_i / \partial x_j$ and $Re > 0$ is the Reynolds number. The flow is influenced by blowing and suction at the control boundary Γ_c according to:

$$\mathbf{y} = \mathbf{u} \quad \text{on } \Sigma_c, \tag{6c}$$

where $\Sigma_c = (0, T) \times \Gamma_c$ and $\mathbf{u}$ is the control satisfying the incompressibility condition:

$$\int_0^T \int_\Gamma \mathbf{u} \cdot \mathbf{n} \, ds \, dt = 0, \tag{IC}$$

with $\mathbf{n}$ is the outward normal on Γ. We henceforth set $U = L^2(\Sigma_c)$ endowed with the common L^2-norm. At $t = 0$ the initial condition

$$\mathbf{y}(0, \mathbf{x}) = \mathbf{y}_\circ(\mathbf{x}), \quad \text{for all } \mathbf{x} \in \Omega, \tag{6d}$$

is imposed, where $\mathbf{y}_\circ$ is a given function on Ω. On the rest of the boundary we prescribe inhomogeneous Dirichlet conditions

$$\mathbf{y} = \mathbf{g} \quad \text{on } \Sigma \setminus \Sigma_c, \tag{6e}$$

where $\mathbf{g}$ is a fixed function satisfying

$$\int_0^T \int_\Gamma \mathbf{g} \cdot \mathbf{n} \, \mathrm{d}s \, \mathrm{d}t = 0,$$

and $\Sigma = (0, T) \times \Gamma$.

Next we specify the cost functional, which results from the discussion in Section 1. For positive scalars β and q we define

$$J(\mathbf{y}, \mathbf{u}) = J_1 + J_2 + J_3, \tag{7a}$$

$$J_1(\mathbf{y}, \mathbf{u}) = \int_0^T \int_{\Omega_o} h(\det \nabla \mathbf{y}) \, \mathrm{d}\mathbf{x} \, \mathrm{d}t, \tag{7b}$$

$$J_2(\mathbf{y}, \mathbf{u}) = \frac{\beta}{2} \int_0^T \int_{\Gamma_c} \mathbf{u}^2 \, \mathrm{d}\mathbf{x} \, \mathrm{d}t, \tag{7c}$$

$$J_3(\mathbf{y}, \mathbf{u}) = \frac{q}{2} \int_0^T \left(\int_{\Gamma_c} \mathbf{u} \cdot \mathbf{n} \, \mathrm{d}\Gamma_c \right)^2 \mathrm{d}t \tag{7d}$$

with $\Omega_o \subseteq \Omega$ and h as in (5). Here J_3 penalizes the deviation of the flow from the incompressibility condition (IC).

The optimal control problem that we consider has the form

$$\min J(\mathbf{y}, \mathbf{u}) \quad \text{such that} \quad (\mathbf{y}, p, \mathbf{u}) \text{ solves (6).} \tag{P}$$

Let $(\mathbf{y}^*, p^*, \mathbf{u}^*)$ denote a local solution to (P). Such a solution must satisfy the first order optimality conditions, referred to as the optimality system. To formally derive this system we introduce

$$\mathcal{L}(\mathbf{y}, p, \mathbf{u}, \boldsymbol{\xi}, \pi) = J(\mathbf{y}, \mathbf{u}) + \int_0^T \int_\Omega \left(\mathbf{y}_t - \frac{1}{Re} \Delta \mathbf{y} + (\mathbf{y} \cdot \nabla)\mathbf{y} + \nabla p \right) \boldsymbol{\xi} \, \mathrm{d}\mathbf{x} \, \mathrm{d}t$$
$$+ \int_0^T \int_\Omega \pi \, \mathrm{div}\, \mathbf{y} \, \mathrm{d}\mathbf{x} \, \mathrm{d}t + \int_0^T \int_{\Gamma_c} (\mathbf{y} - \mathbf{u}) \boldsymbol{\mu} \, \mathrm{d}\Gamma_c \, \mathrm{d}t.$$

Taking derivatives with respect to $\mathbf{y}, p, \mathbf{u}, \boldsymbol{\xi}, \pi$ we obtain the optimality system in the primal variables $(\mathbf{y}, p, \mathbf{u})$ and the adjoint variables $(\boldsymbol{\xi}, \pi)$, where for convenience we drop the superscripts *:

$$\mathbf{y}_t - \frac{1}{Re} \Delta \mathbf{y} + (\mathbf{y} \cdot \nabla)\mathbf{y} + \nabla p = 0 \quad \text{in } Q, \tag{8a}$$

$$-\mathrm{div}\, \mathbf{y} = 0 \quad \text{in } Q, \tag{8b}$$

$$\mathbf{y} = \mathbf{g} \quad \text{on } \Sigma \setminus \Sigma_c, \tag{8c}$$

$$\mathbf{y}(0, \cdot) = \mathbf{y}_\circ \quad \text{on } \Omega, \tag{8d}$$

$$-\boldsymbol{\xi}_t - \frac{1}{Re} \Delta \boldsymbol{\xi} + (\nabla y)^{\mathrm{T}} \boldsymbol{\xi} - (\mathbf{y} \cdot \nabla)\boldsymbol{\xi} + \nabla \pi = -J_{\mathbf{y}} \quad \text{in } Q, \tag{8e}$$

$$-\mathrm{div}\, \boldsymbol{\xi} = 0 \quad \text{in } Q, \tag{8f}$$

$$\boldsymbol{\xi} = 0 \quad \text{on } \Sigma, \tag{8g}$$

$$\boldsymbol{\xi}(T, \cdot) = 0 \quad \text{in } \Omega, \tag{8h}$$

$$\frac{1}{Re} \frac{\partial \boldsymbol{\xi}}{\partial \mathbf{n}} + \boldsymbol{\mu} = \pi \mathbf{n} \quad \text{in } U, \tag{8i}$$

where $J_{\mathbf{y}}$ is the directional derivative of J with respect to $\mathbf{y}$. Introducing the reduced cost functional $\hat{J}: U \to \mathbb{R}$ by

$$\hat{J}(\mathbf{u}) = J\big(\mathbf{y}(\mathbf{u}), \mathbf{u}\big),$$

where $\mathbf{y}(\mathbf{u})$ solves (6) for the control $\mathbf{u} \in U$, we obtain from (8) that the gradient of the reduced cost functional at $\mathbf{u}$ in direction $\delta\mathbf{u} \in U$ is given by

$$\big\langle \hat{J}'(\mathbf{u}), \delta\mathbf{u} \big\rangle_U = \int_0^T \int_{\Gamma_c} \left(\beta\mathbf{u} + \frac{1}{Re}\frac{\partial \boldsymbol{\xi}}{\partial \mathbf{n}} - \pi\mathbf{n} + \mathbf{n}q\left(\int_{\Gamma_c} \mathbf{u}\cdot\mathbf{n}\,\mathrm{d}\Gamma_c \right) \right) \delta\mathbf{u}\,\mathrm{d}\Gamma_c\,\mathrm{d}t, \tag{9}$$

where $\boldsymbol{\xi}$ is computed from (8).

Our numerical approach is based on the reduced problem

$$\text{minimize } \hat{J}(\mathbf{u}) := J\big(\mathbf{y}(\mathbf{u}), \mathbf{u}\big) \quad \text{over } \mathbf{u} \in U, \tag{10}$$

where $\mathbf{y}$ corresponds to the solution of (6). Problem (10) is solved by a Polak–Ribiere type conjugate gradient algorithm (CG-algorithm) combined with a Wolfe–Powell line search procedure [17] for computing appropriate step-sizes along the CG search direction in every iteration.

Based on the error analysis and the arguments given in [18] we used the conditions

$$\big|\hat{J}(\mathbf{u}^k) - \hat{J}(\mathbf{u}^{k-1})\big| \leqslant \epsilon_{\hat{J}}\big(1 + \big|\hat{J}(\mathbf{u}^k)\big|\big), \tag{11}$$

$$\big\|\mathbf{u}^k - \mathbf{u}^{k-1}\big\|_U \leqslant \sqrt{\epsilon_{\hat{J}}}\big(1 + \|\mathbf{u}^k\|_U\big) \tag{12}$$

for termination of the CG-algorithm.

3. Numerical results

Here we present a numerical example by which the applicability of the proposed method for boundary control is tested. As a test example we chose the flow in a 2D lid-driven cavity [19,20] illustrated in Fig. 1. This flow has unambiguous and easy to pose boundary conditions and possesses important features of a real flow: boundary layers, core vortex and secondary vortices. These features are illustrated in Fig. 2(a) by a stream function (Ψ) and velocity vectors plot for $Re = 400$. The flow occupies the region $\Omega = (0,1) \times (0,1)$. Most of the cavity is occupied by the primary vortex (PV) which is driven by the moving lid. The PV induces the bottom-left (BL) and bottom-right (BR) vortices. These vortices are also illustrated in Fig. 2(b) by a contour plot of $\det \nabla\mathbf{y}$.

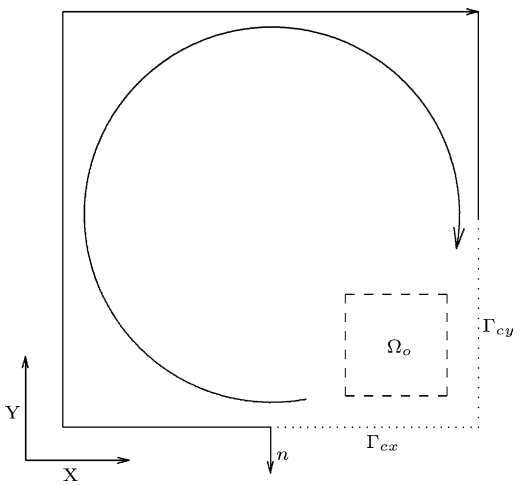

Fig. 1. Sketch of the Lid driven cavity flow together with the observation domain (Ω_o), control boundary ($\Gamma_c = \Gamma_{cx} \cup \Gamma_{cy}$) and the unit outward normal (n).

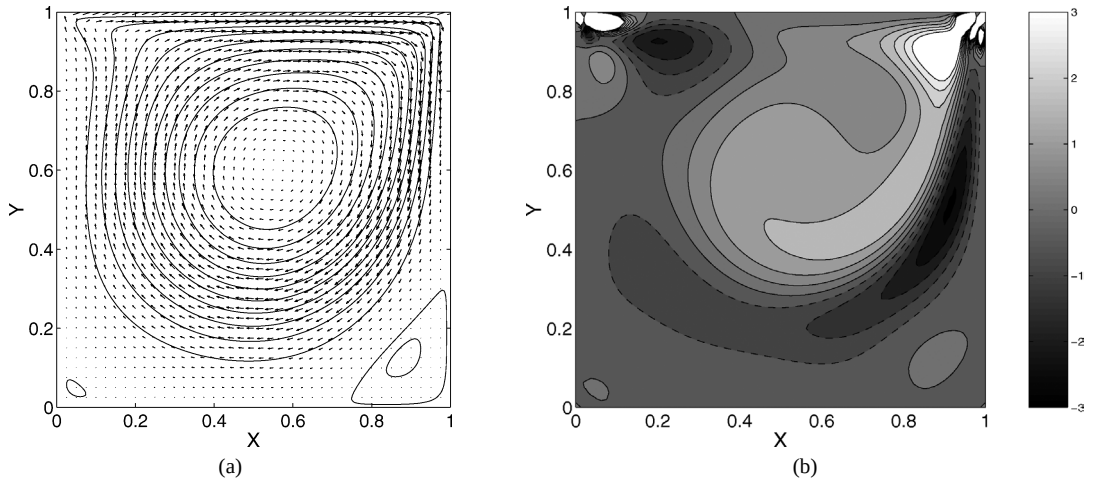

Fig. 2. Lid-driven cavity flow at $Re = 400$: (a) Stream function and velocity vectors; (b) Levels of $\det \nabla \mathbf{y}$. Note that in the oval regions near the bottom corners $\det \nabla \mathbf{y} > 0$.

3.1. Discretization

The controlled Navier–Stokes (6a) and continuity (6b) equations are discretized in space by means of a staggered-grid control-volume approach [21] on a uniform grid. A fifth-order upwind finite difference scheme is applied to the convection terms whereas a fourth-order centered scheme is used for the diffusion terms. The fluxes across the control volume faces are calculated using the mid-face value of the corresponding variable, which results in an overall second order space discretization. Continuity is enforced through a SIMPLE-like scheme [21] where a discrete Poisson equation is iteratively solved by means of the conjugate gradient method [22]. An explicit first order Euler scheme is used to integrate the discrete momentum conservation equations in time. The adjoint equations (8e) and (8f) are solved using the same approach, accounting for the fact that the time integration is backwards in time. The time step is chosen small enough to guarantee both time accuracy and convergence of the solutions of the primal and adjoint systems.

Before going on, we present some results to check the solution of (8) with boundary control. The solution of the primal system (6) is validated in [9] by comparing our results with results from [19]. A standard check of the solution of the optimality system (8) is to track the flow in Ω_o to Stokes flow. In this case:

$$J_1(\mathbf{y}) = \int_0^T \int_{\Omega_o} |\mathbf{y} - \mathbf{y}_{\text{Stokes}}|^2 \, \mathrm{d}\mathbf{x} \, \mathrm{d}t,$$

where $\Omega_o = (0.85, 1) \times (0, 0.15)$ and $\Gamma_c = \Gamma_{cx} \cup \Gamma_{cy}$ (here $\Gamma_{cx} = [0.5, 1]$ and $\Gamma_{cy} = [0, 0.5]$ are the portions of the control boundary parallel to the X and Y directions, respectively, see Fig. 1). Fig. 3(a) presents a zoom of the velocity vectors in the BR corner of the uncontrolled flow for $Re = 400$, $T = 5$ while Fig. 3(b) presents the target flow (the Stokes flow). The control action shown in Fig. 3(d) prevents the counterclockwise motion of the flow in Ω_o which is not present in the Stokes flow.

3.2. Reduction of the BR vortex

Our control objective is to reduce the BR vortex by means of blowing and suction at the cavity walls. For this purpose we consider the control boundary and observation domain to be Γ_c as defined above and $\Omega_o = (0.75, 0.95) \times (0.05, 0.2)$, respectively.

Before presenting the numerical results we give the values of some parameters used in the numerical solution of the optimality system. The stopping tolerance $\epsilon_{\hat{J}}$ is chosen in such a way that further iterations do not lead to significant changes in $\mathbf{u}$ and $\mathbf{y}$. For the results presented in this paper $\epsilon_{\hat{J}} = 10^{-6}$. For this tolerance level the values of J_2 are

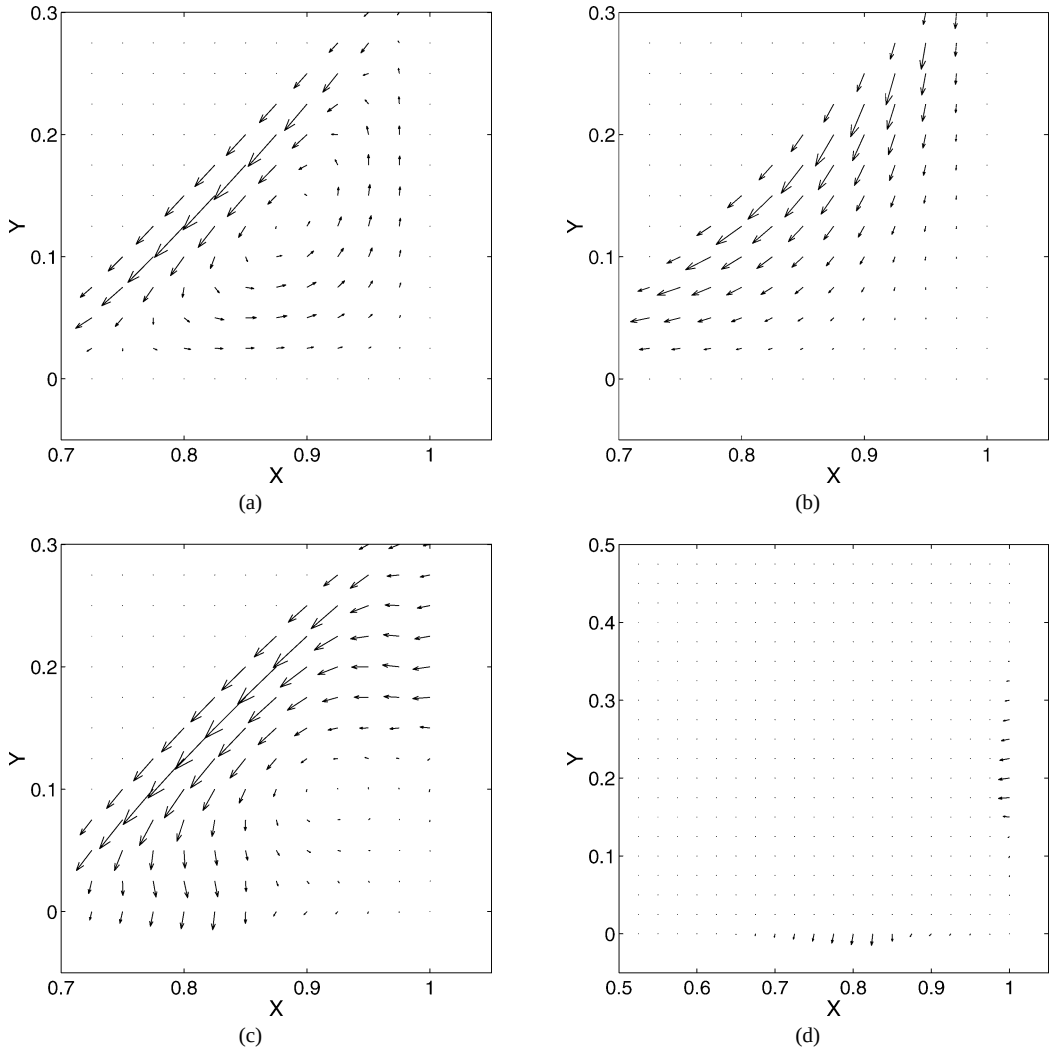

Fig. 3. Boundary control. Tracking to Stokes flow for $Re = 400$ and $T = 5$. Here $\Omega_o = (0.85, 1) \times (0, 0.15)$. (a) Velocity vectors of the uncontrolled flow; (b) Velocity vectors of the target flow; (c) Velocity vectors of the controlled flow at $t = 4$; (d) Control action at $t = 4$. Note that the velocities outside of the bottom-left corner are padded with zeros purely for visualization purposes.

around 10^{-4} and the iteration terminates with $\|\mathbf{u}_k - \mathbf{u}_{k-1}\|_U \leqslant 1.15 \times 10^{-3}$ and $\|\mathbf{u}_k\|_U \approx 0.15$. If $\epsilon_{\hat{J}} = 10^{-4}$ we still obtain good convergence and the iteration stops with $\|\mathbf{u}_k - \mathbf{u}_{k-1}\|_U \leqslant 1.15 \times 10^{-2}$.

The value of the penalty parameter is fixed to $q = 100$ for all the calculations. For this value of q, $J_3 < 10^{-7}$ which implies a good satisfaction of the incompressibility condition. Smaller values of q are also tested and for example for $q = 1$, $J_3 < 10^{-6}$. No significant difference between the results for these values of q is observed.

The time horizon is fixed to $T = 5$ for all the numerical examples if not stated otherwise. The regularization parameter δ takes a value $\delta = 10^{-4}$ which approximately corresponds to the accuracy of the discretization for the grids used. Values $0 \leqslant \delta \leqslant 10^{-3}$ are also tested but no significant differences in the results are found.

A typical value for the cost-parameter is $\beta = 10^{-2}$. In this case J_1 and βJ_2 are of approximately the same order at the converged values. Results for $Re = 400$, grid resolution 41×41, and time step 0.015 are presented in Fig. 4. It should be noted that in this case the CG method is initiated with a zero control guess for the first iteration. The velocity vectors of the uncontrolled flow in the region of the BR vortex are the same as those in 3(a). We monitored the values of J and $\|\nabla J\|$ during the iteration and confirmed that they are decreasing. The contour plots of $\det(\nabla \mathbf{y})$ presented in Figs. 4(a)–(b) show again the reduction of $\det(\nabla \mathbf{y})$ in Ω_o when control is applied. The blowing/suction action near the end of the time horizon ($t = 4$) is shown in Fig. 4(c). It can be seen that the control tries to counteract

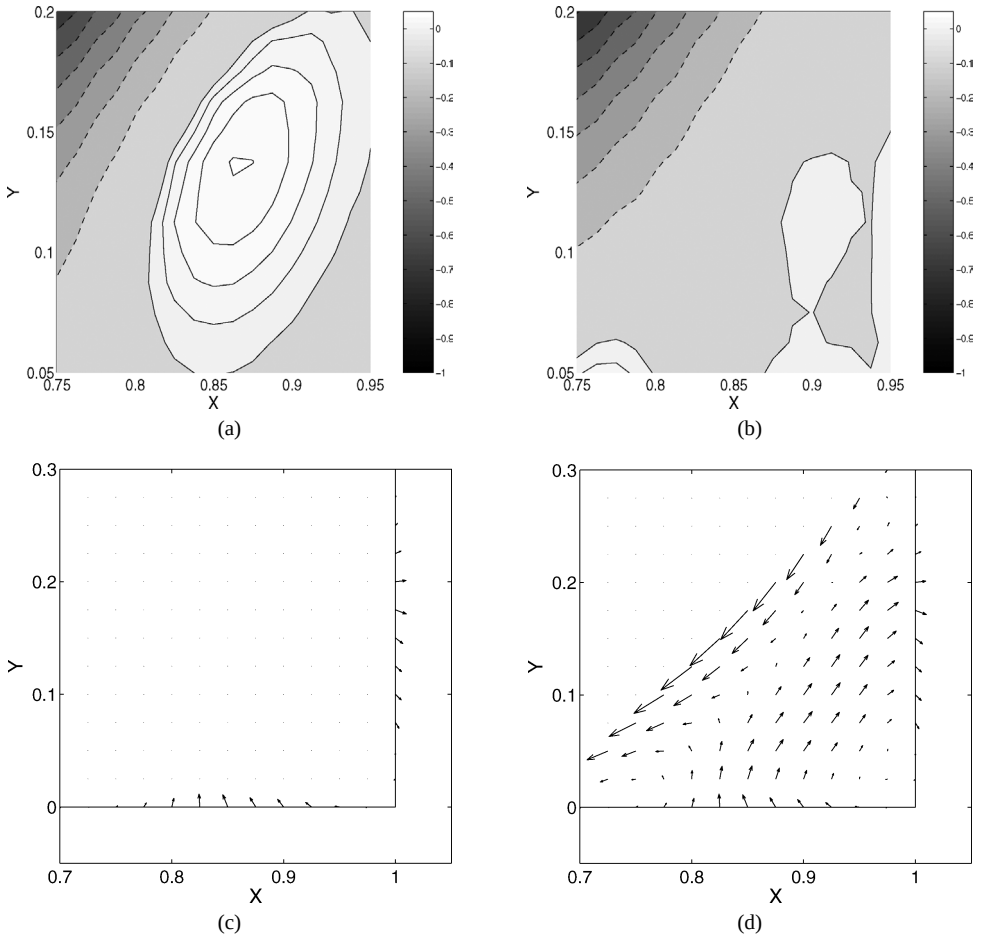

Fig. 4. Boundary control using $\det(\nabla \mathbf{y})$. Results for $Re = 400$ and $T = 5$. (a) Contour plot of $\det(\nabla \mathbf{y})$ for the uncontrolled flow; (b) Contour plot of $\det(\nabla \mathbf{y})$ for the controlled flow at $t = 4$; (c) Control action at $t = 4$; (d) Velocity vectors of the controlled flow at $t = 4$; Notes: the velocities outside of the bottom-left corner in (d) are padded with zeros purely for visualization purposes; The dashed contour levels correspond to negative values and the continuous ones to positive values.

the BR vortex. The controlled flow shown in Fig. 4(d) shows that the BR vortex is suppressed by injecting fluid from the lower wall (mostly in the region $(0.7, 1)$) and sucking from the vertical wall (mostly in the region $(0, 0.2)$). This at first glance unexpected direction of the blowing/suction direction motivated us to perform two additional tests starting the CG method from different initial guesses. The CG method is initialized with time independent control with $u_1|_{\Gamma_c} = u_2|_{\Gamma_c} = \pm 0.01$ and the results are shown in Fig. 5. The idea behind the initialization with the $-$ sign lies in the intuitive expectation that the control should blow from the vertical wall and suck from the horizontal wall and thus sweep out the BR vortex. The resulting controlled flows at $t = 4$ are shown in Fig. 5(a) and (c) and the corresponding controls in Figs. 5(b) and 5(d) for the $-$ and $+$ sign, respectively. It can be seen that the BR vortex is swept out in both cases. The convergence history for these cases (not presented here) shows a smaller decrease for J and J_1 than for the case with zero control as an initial guess. This motivated us to initialize the CG iterations with zero control for the subsequent simulation.

We further checked the performance of the method for a higher value of the Reynolds number, namely $Re = 1000$. It should be noted that we obtained a significantly better decrease in J when initializing the CG iteration with the control obtained for $Re = 400$ and therefore we present these results in Fig. 6. The contour plots of $\det(\nabla \mathbf{y})$ presented in Figs. 6(a)–(b) show again the reduction of $\det(\nabla \mathbf{y})$ in Ω_o. The blowing/suction action near the end of the time horizon ($t = 4$) is shown in Fig. 6(e). It can be seen that the control tries to counteract the BR vortex. The controlled flow shown in Fig. 6(f) shows that the BR vortex is suppressed when judged by the velocity field.

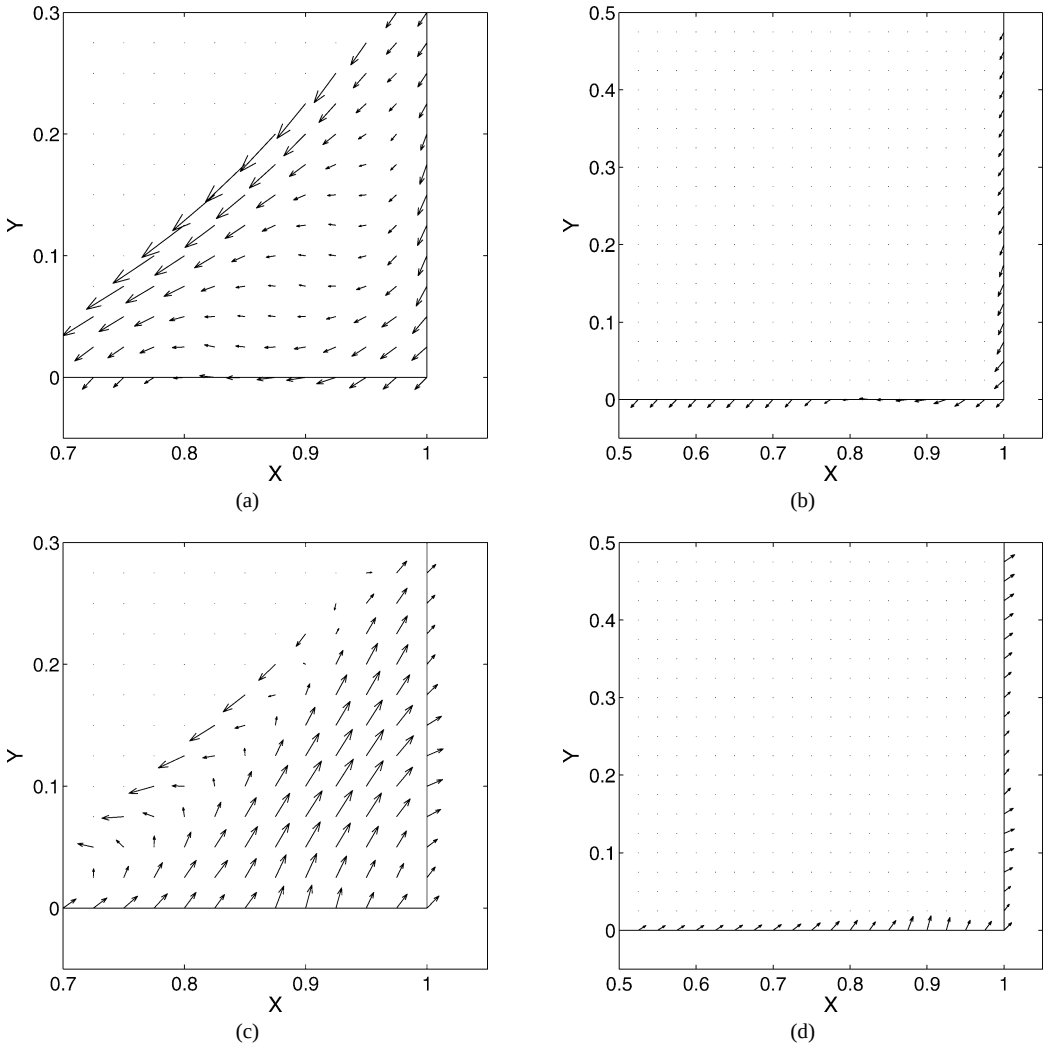

Fig. 5. Boundary control using $\det(\nabla \mathbf{y})$. Results for $Re = 400$, $T = 5$ and $t = 4$. The CG method is initialized with a time independent control ($u_1|_{\Gamma_c} = u_2|_{\Gamma_c} = \pm 0.01$). (a) Velocity vectors of the controlled flow for the $-$ sign; (b) Control action for the $-$ sign; (c) Velocity vectors of the controlled flow for the $+$ sign; (d) Control action for the $+$ sign. Note that the velocities outside of the bottom-left corner are padded with zeros purely for visualization purposes.

4. Conclusions

Based on definitions for vorticity involving the velocity gradient tensor we proposed an optimal control formulation for boundary control of vortices in incompressible fluid flow. The optimality system was characterized and an iterative numerical solution procedure was proposed. The effectiveness of the formulation was demonstrated for the model problem of cavity flow with blowing/suction along parts of the boundary. A comparison to the well established optimal control formulation based on tracking to the Stokes flow is provided as well. We believe the results encourage further investigations including three-D flows, flows involving more complex geometries and flow patterns. Let us also recall that the quantification of "vorticity" is not fully settled and this in turn will have impact on the proper optimal control formulation. From the mathematical and optimization point of view the cost functionals which arise from different quantifications of vorticity given in the literature offer interesting new challenges including, for example, the development of sufficient optimality conditions and sensitivity analysis with respect to the geometry of the flow region.

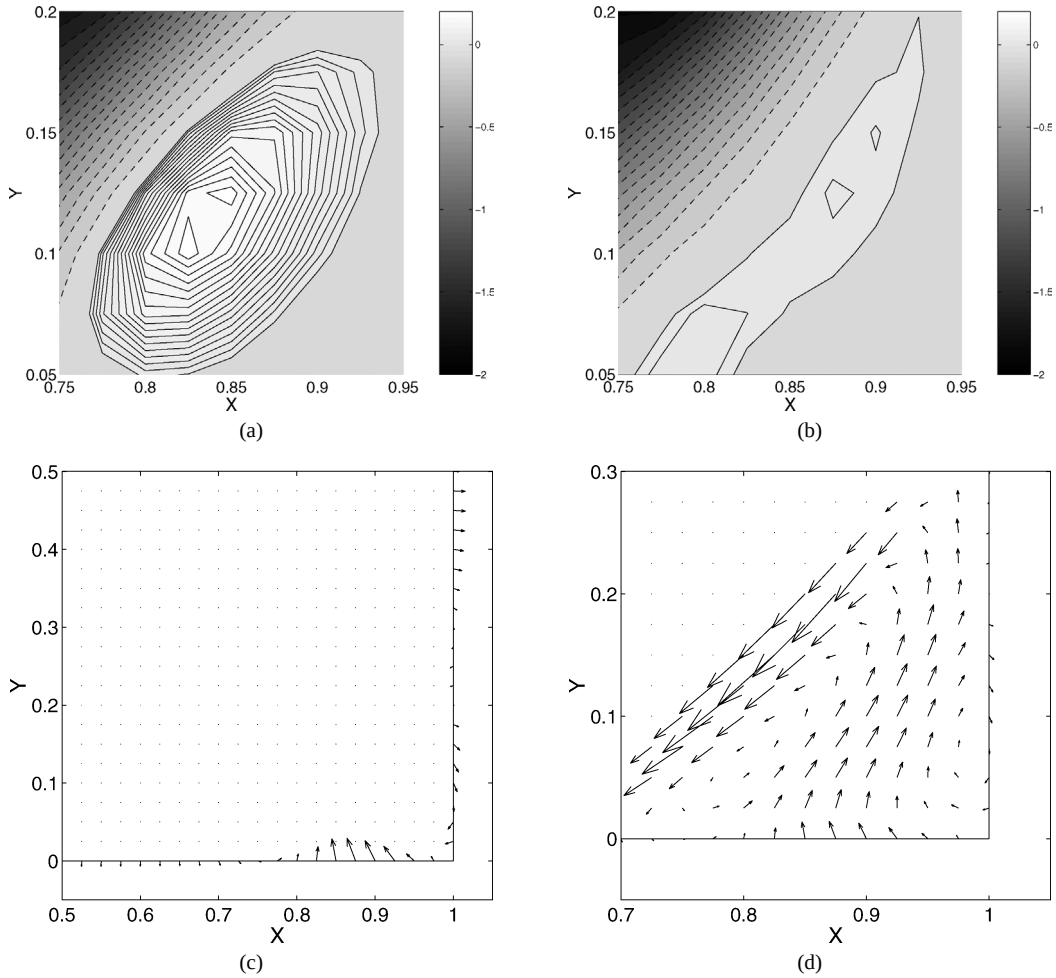

Fig. 6. Boundary control using $\det(\nabla \mathbf{y})$. Results for $Re = 1000$ and $T = 5$. The CG method is initialized with the control obtained for $Re = 400$. (a) Contour plot of $\det(\nabla \mathbf{y})$ for the uncontrolled flow; (b) Contour plot of $\det(\nabla \mathbf{y})$ for the controlled flow at $t = 4$; (c) Control action at $t = 4$; (d) Velocity vectors of the controlled flow at $t = 4$; Note that the velocities outside of the bottom-left corner are padded with zeros purely for visualization purposes. The dashed contour levels correspond to negative values and the continuous ones to positive values.

References

[1] M.S. Chong, A.E. Perry, B.J. Cantwell, A general classification of three-dimensional flow fields, Phys. Fluids A 2 (1990) 765–777.
[2] H.M. Blackburn, N.N. Monsour, B.J. Cantwell, Topology of fine-scale motions in turbulent channel flow, J. Fluid Mech. 310 (1996) 293–324.
[3] W. Kaplan, Ordinary Differential Equations, Addison-Wesley Publ. Comp., Reading, MA, 1967.
[4] J.C.R. Hunt, A.A. Wray, P. Moin, Eddies, stream and convergence zones in turbulent flows, Center for Turbulence Research Report, CTR-S88, p. 193.
[5] J. Jeong, F. Hussain, On the identification of a vortex, J. Fluid Mech. 85 (1995) 69–94.
[6] A. Obkubo, Horizontal dispersion of floatable trajectories in the vicinity of velocity singularities such as convergencies, Deep-Sea Res. 17 (1970) 445–454 (McGraw-Hill, 1980).
[7] J. Weiss, The dynamics of enstrophy transfer in 2-dimensional hydrodynamics, Physica D 48 (1991) 273–294.
[8] G. Haller, An objective definition of a vortex, J. Fluid Mech., in press.
[9] M. Hintermüller, K. Kunisch, Y. Spasov, S. Volkwein, Dynamical systems based optimal control of incompressible fluids, Int. J. Numer. Methods Fluids 4 (2004) 345–359.
[10] F. Abergel, R. Temam, On some control problems in fluid mechanics, Theoret. Comput. Fluid Dynamics 1 (1990) 303–325.
[11] T.T. Bewley, Flow control: new challenges for a new Renaissance, Progr. Aerospace Sci. 37 (2001) 21–58.
[12] E. Casas, Optimality conditions for some control problems of turbulent flows, in: M. Gunzburger (Ed.), Flow Control, Springer-Verlag, Berlin, 1995.
[13] M. Gunzburger (Ed.), Flow Control, Springer-Verlag, New York, 1995.
[14] H. Choi, M. Hinze, K. Kunisch, Instantaneous control of backstep-facing step flows, Appl. Numer. Math. 31 (1999) 133–158.

[15] M. Desai, K. Ito, Optimal control of Navier–Stokes equations, SIAM J. Control Optim. 32 (1994) 1428–1446.
[16] K. Kunisch, S. Volkwein, L. Xie, HJB-POD based feedback design for the optimal control of evolution problems, SIAM J. Appl. Dynamical Systems 4 (2004) 701–722.
[17] J.J. Moré, D.C. Sorensen, Newton's method, in: G.H. Golub (Ed.), Studies in Numerical Analysis, The Mathematical Association of America, 1984, pp. 29–82.
[18] P.E. Gill, W. Murray, M.H. Wright, Practical Optimization, Academic Press, San Diego, 1981.
[19] U. Ghia, K.N. Ghia, C.T. Shin, High-Re solutions for incompressible flow using the Navier–Stokes equations and a multigrid method, J. Comput. Phys. 48 (1982) 387.
[20] E. Leriche, S. Gavrilakis, Direct numerical simulation of the flow in a lid-driven cavity flow, Phys. Fluids 12 (2000) 1363.
[21] S.V. Patankar, Numerical Heat Transfer and Fluid Flow, McGraw-Hill, 1980.
[22] G.H. Gollub, Ch.F. Van Loan, Matrix Computations, third ed., The Johns Hopkins University Press, Baltimore, MD, 1996.